RESEARCH PAPER

Multi-herbal combinatorial strategy: Enhanced antidermatophytic activity of plant- extract combinations against clinically important *Microsporum* spp.

Mrinalini Devi U.G.[1], Sushma H.N, *Sharmila T*[1]
[1] Department of Microbiology, Bangalore University, Bengaluru 560056, Karnataka, India
Corresponding author: Mrinalini Devi U.G*, mrinaliniug@gmail.com; ORCID I.D: 0000-0003-1856-1204
Co-authors: Sharmila T. (sharmila1966@yahoo.co.in); Sushma H.N. (sushmahn1993@gmail.com)

Abstract
Background: Skin and nail dermatophytic infections are common. Dermatophytes are contagious fungi that infect the keratinized tissues of humans and animals superficially, and the group is distinguished by its capacity to break down keratin. *Microsporum canis*, which causes dermatophytosis in people and cats, is frequently encountered in clinical settings and is challenging to treat, especially in immunocompromised individuals. Existing antimycotics have a number of limitations: emerging antifungal resistance, adverse effects and toxicity, drug interactions, chronic recurrent dermatophytosis and prolonged treatment. Combining medicinal plant extracts is a promising route to cost-effective, patient-friendly alternatives, and a synergistic interaction is the outcome most worth seeking.
Aim: The present study aimed to evaluate the *in vitro* antidermatophytic activity and synergistic interactions of combinatorial crude plant extracts against *Microsporum gypseum* and *Microsporum canis*.
Materials and Methods: Crude extracts prepared from the leaves of *Calotropis procera*, *Syzygium cumini*, *Mangifera indica* and *Senna siamea*, and from the pods of *Senegalia rugata*, were evaluated in combinations of two, three and four extracts at fixed ratios. Antidermatophytic activity was assessed by disc diffusion and by broth microdilution in 96-well microtiter plates. Minimum inhibitory concentrations (MIC) were determined, and interactions were classified with the fractional inhibitory concentration index (FICI). The two synergistic combinations were profiled by GC–MS; their constituents were then docked against a fungal target protein, screened *in silico* for drug-likeness and toxicity, and tested for cytotoxicity on HaCaT keratinocytes by MTT assay.
Results: No combination was synergistic against *M. gypseum*, even though *S. cumini* + *C. procera* + *S. rugata* (0.5:0.5:0.5) gave the largest inhibition zone of the study (26.6 ± 2.8 mm). Against *M. canis*, two combinations were synergistic: *S. rugata* + *M. indica* (0.5:0.5; 17.0 ± 0.7 mm; MIC 1,250 µg/mL) and *C. procera* + *S. rugata* + *M. indica* (0.5:1:1; MIC 312 µg/mL). Adding more plants did not raise activity; median zones against *M. canis* were 14.8, 10.2 and 14.4 mm for two-, three- and four-extract combinations. Lupeol (14.26%) and phytol (13.49%) dominated the GC–MS profile of combination 2, and stigmasterol showed the strongest predicted binding (−11.0 kcal/mol). Both combinations inhibited HaCaT growth (IC_{50} 91.76 µg/mL for combination 1) at concentrations below their antifungal MICs.
Conclusion: Combinatorial herbal extracts possess enhanced antidermatophytic potential against *M. canis*. Synergy depended on the composition and proportion of the extracts and on the fungal species, not on the number of plants. The narrow gap between keratinocyte cytotoxicity and antifungal MIC means the crude combinations need fractionation before they can be developed as topical therapeutics.
Keywords: Dermatophytes; Tinea; *Microsporum canis*; *Nannizzia gypsea*; Combination studies; Fractional inhibitory concentration index; GC–MS; Molecular docking
How to cite this article: Mrinalini Devi U.G.1 Sushma H.N Sharmila T*1. Multi-herbal combinatorial strategy: Enhanced antidermatophytic activity of plant- extract combinations against clinically important Microsporum spp.. Int J Drug Deliv Technol. 2026;16(90s):643-660. DOI: 10.25258/ijddt.16.90s.63.

Introduction

Dermatophytes are among the most common fungal pathogens, responsible for superficial infections of the skin, hair and nails worldwide [1–3]. These fungi belong to the family Arthrodermataceae (order Onygenales, class Eurotiomycetes, phylum Ascomycota). *Trichophyton*, *Epidermophyton*, *Nannizzia*, *Paraphyton*, *Lophophyton*, *Microsporum* and *Arthroderma* are the seven genera that contain the clinically relevant dermatophytes [4, 5]. Although dermatophytes occur freely in the environment, they cause infection in humans and animals only under specific conditions [6]. They produce septate, hyaline, filamentous hyphae and asexual spores. Depending on the species and environmental conditions, the conidia may be microconidia (small, unicellular), macroconidia (large, multi-septate) or arthroconidia (formed by fragmentation of hyphae), and these structures aid identification and classification [4].

About 20–25% of people worldwide develop fungal infections of the skin and nails, especially in tropical and subtropical regions,

where humidity and warm temperatures favour skin infection [2]. Dermatophytes are keratinophilic fungi that proliferate rapidly and infiltrate keratin-rich tissues such as skin, hair and nail. Certain species live as saprobes on fragments of feathers, nails and hair in the soil, while anthropophilic species can colonize humans without inducing lesions in the integument. Sulfite-mediated cleavage of the disulfide bonds in keratin, together with secreted proteases, allows these fungi to degrade and use keratinous substrates [7].

The most prevalent dermatophytes include *Microsporum canis* (*M. canis*), *Trichophyton rubrum*, *Trichophyton benhamiae* and *Trichophyton tonsurans* [8]. The genus *Microsporum* is clinically significant because of its high probability of causing disease in both humans and animals, and *M. canis* is the main agent of feline dermatophytosis, from which it passes to people [8, 9]. *Microsporum gypseum*, a geophilic species now placed in the genus *Nannizzia* as *N. gypsea* [4], is retained here under its former name to match the culture-collection designation of the strain. In certain cases, hairs infected with *M. canis* and *M. gypseum* may show green to yellow-green fluorescence under Wood's lamp examination [10].

However, adverse effects, limited therapeutic options, drug–drug interactions and the emergence of resistance to the available antifungal classes (azoles, polyenes, echinocandins and pyrimidine analogues) all complicate the management of fungal infections [11, 12]. The phytochemistry of numerous plant species suggests that phytochemicals may be a useful source of antifungal treatment alongside synthetic drugs [13, 14]. Plant extracts used in combination offer an advantage: the diverse phytochemicals they contain can interact through synergistic or additive mechanisms and act on different cellular targets, so their combined effect may exceed that of individual constituents. Such interactions may also be antagonistic, and only experimental evaluation can tell which [15]. Resistance is also less likely to arise against a mixture of bioactive substances than against a single active molecule [16].

Systematic, quantitative studies of combinations of two or more crude medicinal-plant extracts against

M. canis and *M. gypseum* remain scarce [17]. The present study therefore evaluated the *in vitro* antidermatophytic activity of combinations of crude extracts prepared from the leaves of *Calotropis gigantea*, *Syzygium cumini*, *Mangifera indica* and *Senna siamea* and from the pods of *Senegalia rugata* against both species. Combinations of two, three and four extracts were studied, and the FICI was calculated to identify synergistic, additive, indifferent or antagonistic interactions. The individual extracts were assessed for antidermatophytic activity in a prior study (18); the current work builds on it by testing selected combinations and quantifying their interactions. The synergistic combinations were then characterised chemically by GC–MS, their constituents were docked against a fungal target protein and screened for drug-likeness and predicted toxicity, and the combinations were tested for cytotoxicity on human keratinocytes.

Materials and Methods

The overall experimental workflow is summarised in Figure 1.

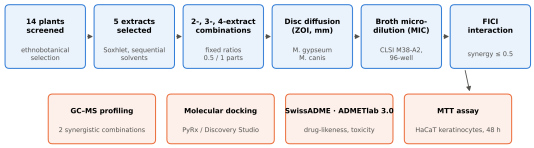

Figure 1. Experimental workflow. Five of fourteen screened plants were extracted and combined at fixed ratios; combinations were tested by disc diffusion and broth microdilution against *M. gypseum* and *M. canis*, and interactions were classified by FICI. The synergistic combinations were analysed by GC–MS, molecular docking, *in silico* ADMET screening and MTT cytotoxicity on HaCaT keratinocytes.

Chemicals and reagents

All reagents and chemicals used in this study were of analytical grade and procured from HiMedia Laboratories Pvt. Ltd., Mumbai, India. Glassware was obtained from Borosil, India.

Collection and authentication of plant materials

Fourteen angiosperm species were selected on the basis of ethnobotanical relevance, namely *Piper longum*(RRCB1-5418), *Plectranthus amboinicus*(RRCBI-mus214), *Mangifera indica*(RRCBI-musl 10), *Senna siamea*(RRCBI-19156)., *Senegalia rugata*(RRCBI-5736), *Curcuma longa*(RRCBI-mus277), *Nerium oleander*(RRCBI-15290), *Ficus racemosa(*(RRCB1-8021).*Eucalyptus globulus(*(RRCBI-17965), *Calotropis gigantea(*(RRCB1-8770), *Trigonella foenum-graecum*((RRCB1-mus105). *Azadirachta indica*(RRCB1-8970), *Piper betle* (RRCB1-musl 13)and *Syzygium cumini*(RRCB1-5418). Plant materials were collected from the university campus and surrounding regions of Bengaluru, Karnataka, India, and were

authenticated by taxonomists of the Central Council for Research in Ayurvedic Sciences (CCRAS), Bengaluru). Based on preliminary screening, the five plants with maximum antidermatophytic activity were selected for further work: *Senegalia rugata* (syn. *Acacia concinna*), *Senna siamea*, *Syzygium cumini*, *Mangifera indica* and *Calotropis gigantea.*

Preparation of plant extracts

Fresh plant parts were washed thoroughly, shade-dried and powdered in an electric grinder. Sequential hot extraction was then performed in a Soxhlet apparatus with solvents of increasing polarity (hexane, ethyl acetate, methanol and ethanol). Approximately 60 g of powdered material was extracted with 300 mL of each solvent for 72 hr. Extracts were concentrated on a rotary evaporator and stored at 4 °C. The ethanolic/ methanoliccrude extracts of *S. rugata*, *M. indica*, *S. cumini*, *C. gigantea* and *S. siamea* were used to prepare two-, three- and four-extract combinations in predetermined ratios, where 0.5 and 1 denote the relative parts of each extract in the mixture.

Fungal strains and culture maintenance

Microsporum gypseum (MTCC 3270) and *Microsporum canis* (MTCC 2829) were obtained from the Microbial Type Culture Collection (MTCC), Chandigarh, India. Cultures were maintained on Sabouraud dextrose agar (SDA; HiMedia, India) slants and plates at 30 °C, and master cultures were preserved as 10% glycerol stocks at 4 °C.

Preparation of fungal inoculum

Inoculum was prepared following CLSI M38-A2 [18] with slight modifications. Five-day-old cultures on SDA were flooded with sterile distilled water containing Tween 20 to obtain conidial suspensions, which were centrifuged at 6,000 rpm for 15 min. The pellet was resuspended in sterile distilled water and vortexed for 15 s, and the turbidity was adjusted to a 0.5 McFarland standard at 530 nm, corresponding to approximately 10^5 CFU/mL.

Antifungal activity by disc diffusion

Antifungal activity was evaluated by the disc diffusion method following CLSI M51-A [19]. Extracts were prepared at 20 mg/mL in 10% dimethyl sulfoxide (DMSO). SDA plates supplemented with chloramphenicol (50 µg/mL) were inoculated with spore suspension by sterile swab. Sterile 6 mm discs were placed on the agar and 10 µL of extract was dispensed onto each disc. Ketoconazole (25 µg/mL) served as the positive control and 10% DMSO as the negative control. Plates were incubated at 28–30 °C for 72–96 h, and zones of inhibition (ZOI) were measured in millimetres. All experiments were done in triplicate. Combinations showing very good activity were taken forward for MIC and FICI evaluation.

Determination of minimum inhibitory concentration

MICs were determined by broth microdilution according to CLSI M38-A2 [18]. Extracts prepared at 50 mg/mL in 10% DMSO were diluted in RPMI-1640 medium as two-fold serial dilutions across the wells to give 3.9–1,000 µg/mL. Each well received 100 µL of standardised inoculum (≈10^4–10^5 CFU/mL). Ketoconazole served as the reference drug and 10% DMSO as the negative control. Plates were incubated at 30 °C for 72 h, and the MIC was taken as the lowest concentration showing no visible fungal growth.

Fractional inhibitory concentration index

The MICs of each extract alone and in combination were determined by broth microdilution. The fractional inhibitory concentration (FIC) of each extract was calculated by dividing its MIC in combination by its MIC alone, and the FIC values of all extracts in a combination were summed to give the FICI:

FICI = Σ (MIC of extract *i* in combination / MIC of extract *i* alone)

Interactions were classified as synergistic (FICI ≤ 0.5), additive (0.5 < FICI ≤ 1.0), indifferent (1.0 < FICI ≤ 4.0) or antagonistic (FICI > 4.0) [16, 20].

Identification of synergistic extract combinations

Crude extracts of *S. rugata*, *M. indica*, *S. cumini*, *C. procera* and *S. siamea* were mixed at predetermined ratios in combinations of two, three and four. Each combination was first screened by disc diffusion against *M. canis* and *M. gypseum*; combinations were then compared on ZOI and MIC, and those with synergistic FICI values were chosen for chemical and *in silico* characterisation.

Gas chromatography–mass spectrometry

Combination 1 (*S. rugata* + *M. indica*, 0.5:0.5) and combination 2 (*C. procera* + *S. rugata* + *M. indica*, 0.5:1:1) were analysed on a Shimadzu GCMS-QP2010 S gas chromatograph–mass spectrometer with GCMS Solution software and an Rtx-5 capillary column. Extracts were diluted 1:100 (v/v) in the appropriate solvent and filtered, and 1 µL was injected in split mode (split ratio 30:1) with the injector at 300 °C. Helium was the carrier gas (1.0 mL/min). The column was held at 60 °C and then programmed to 300 °C, with a 10 min final hold Detection used electron ionisation at 70 eV in full-scan mode

(m/z 40–550). Compounds were identified by comparing their mass spectra with the NIST spectral library, and relative abundance was expressed as percentage peak area.

Molecular docking

Docking was used to examine the molecular complementarity between the GC–MS constituents and a fungal target protein. The crystal structure of (lanosterol 14α-demethylase(CYP51); (PDB ID: 4LXJ) was downloaded from the Protein Data Bank (www.rcsb.org). Non-amino-acid residues (water molecules, ions and co-crystallised ligands) were removed, polar hydrogens were added, and the structure was energy-minimised in Discovery Studio. Ligand structures were obtained from PubChem. Docking was performed in PyRx [21] using the AutoDock Vina engine [22] (Poses with the lowest binding energy were analysed for hydrogen-bond and hydrophobic interactions in Discovery Studio Visualizer.

Drug-likeness and toxicity prediction

Selected constituents were screened for physicochemical properties and Lipinski's rule of five (molecular weight ≤ 500 Da, LogP ≤ 5, hydrogen-bond donors ≤ 5, hydrogen-bond acceptors ≤ 10) [23] with SwissADME [24]. Toxicity endpoints, including hERG blockade, drug-induced liver injury (DILI), AMES mutagenicity, carcinogenicity, skin sensitisation, eye corrosion/irritation and respiratory toxicity, were predicted with ADMETlab 3.0 [25].

MTT cytotoxicity assay

The cytotoxicity of the selected combinations was assessed by the MTT [3-(4,5-dimethylthiazol-2-yl)-2,5-diphenyltetrazolium bromide] assay [26] on the human keratinocyte cell line HaCaT [27]. Metabolically active cells reduce MTT to insoluble purple formazan, and the amount formed, measured at 570 nm, is proportional to the number of viable cells.

HaCaT cells were obtained from the National Centre for Cell Science (NCCS), Pune, India, and maintained in high-glucose Dulbecco's Modified Eagle Medium (DMEM; HiMedia) supplemented with 10% fetal bovine serum and 1% antibiotic–antimycotic solution at 37 °C in a humidified 5% CO_2 atmosphere, with routine subculture at confluence.

Cells were seeded in 12-well plates at 50,000 cells per well and allowed 24 h to adhere. They were then exposed to the combinations at 31.25, 62.5, 125, 250 and 500 µg/mL for 48 h at 37 °C in 5% CO_2. Untreated cells served as the negative control, ketaconazole (1 µM) as the positive control, and medium without cells as the blank. After treatment the medium was removed and MTT was added to a final concentration of 0.5 mg/mL; plates were kept in the dark at 37 °C for 3 h. The MTT medium was removed, formazan was dissolved in DMSO with gentle shaking, and absorbance was read at 570 nm on a microplate reader. Viability was calculated as (absorbance of treated cells / absorbance of untreated control) × 100, and growth inhibition as 100 − viability. The IC_{50} was derived from the concentration–response curve. Cell morphology was recorded by phase-contrast microscopy.

Statistical analysis

All experiments were performed in triplicate and results are expressed as mean ± standard error (SE).. Differences among treatments were analysed by one-way ANOVA followed by Tukey's HSD post-hoc test in SPSS version 20, with $p < 0.05$ considered significant. To compare activity across ratios and across combination sizes, the ratio-level mean ZOIs were summarised as box-and-whisker plots (median, interquartile range and 1.5 × IQR whiskers) in Python (matplotlib). Concentration–response data were fitted with a three-parameter log-logistic model.

Results

Antidermatophytic activity of plant-extract combinations against *Microsporum gypseum*

The antifungal activity of two-, three- and four-extract combinations against *M. gypseum* is presented in Tables 1, 4 and 6. Four of the six two-extract pairs produced no inhibition at any ratio (Table 1; Figure 2a). Among the active pairs, *S. siamea* + *S. rugata* (1:1) and *C. gigantea* + *S. cumini* (0.5:1) gave the highest zones within this group, 12.3 ± 2.0 mm and 12.0 ± 1.5 mm respectively, and both combinations had an MIC of 625 µg/mL.

The three-extract combinations were more active. *S. cumini* + *C. gigantea* + *S. rugata* (0.5:0.5:0.5) produced the largest zone recorded in the whole study, 26.6 ± 2.8 mm, with an MIC of 625 µg/mL (Table 4; Figure 4b). This value stands well apart from the other 28 three-extract readings, whose median was 11.5 mm (Figure 3). In the four-extract group, the largest zone was 18.0 ± 1.0 mm at 1:1:0.5:0.5, and the 0.5:1:1:0.5 ratio taken forward for FICI analysis gave 17.3 ± 1.1 mm with an MIC of 625 µg/mL (Table 6).

FICI analysis did not identify a synergistic interaction for any combination tested against *M. gypseum* (Table 7; Figure 5). One pair was additive and four combinations were indifferent. So, although inhibition zones differed between combinations, the FICI

results do not support classing any of them as synergistic against this organism.

Antidermatophytic activity of plant-extract combinations against *Microsporum canis*

Every two-extract pair inhibited *M. canis* (Table 2; Figure 2b), which contrasts sharply with *M. gypseum*. *S. rugata* + *M. indica* gave its largest zone at 0.5:0.5 (17.0 ± 0.7 mm), with an MIC of 1,250 µg/mL. The single highest two-extract value, however, was *C. gigantea* + *S. cumini* at 1:1 (20.5 ± 0.7 mm).

Among the three-extract combinations, *S.cumini* + *C. gigantea* + *M. indica* at 0.5:0.5:0.5 produced a zone 15.0 ± 0.7 mm and the lowest MIC of any combination, 312 µg/mL. In the four-extract group, the largest zone was 18.0 ± 1.0 mm (1:1:0.5:0.5); the 0.5:0.5:0.5:0.5 ratio used for FICI produced 16.3 ± 0.5 mm with an MIC of 625 µg/mL (Table 5).

FICI analysis identified two synergistic combinations against *M. canis*: the two-extract combination *S. rugata* + *M. indica* (0.5:0.5) and the three-extract combination *C. gigantea*+ *S. rugata* + *M. indica* (0.5:1:1). *S. rugata* + *S. cumini* (0.5:1) was additive, and the remaining combinations were indifferent (Table 7; Figure 5). Both synergistic combinations contain *S. rugata* and *M. indica*. The synergy therefore depended on the composition and proportion of the extracts rather than on the number of plants in a combination.

Effect of combination ratio and combination size

Ratio mattered as much as composition. For a fixed set of three plants, the ZOI against *M. canis* varied by up to 6.5 mm between ratios, and *S. cumini* + *C. gigantea* + *S. rugata* against *M. gypseum* ranged from 10.5 to 26.6 mm (Figure 4). Combination size did not follow a simple "more is better" pattern (Figure 3). Against *M. canis*, median ZOIs across all tested ratios were 14.8 mm (two extracts, n = 24), 10.2 mm (three, n = 28) and 14.4 mm (four, n = 12). Against *M. gypseum*, the two-extract median was 0 mm because most pairs were inactive, rising to 11.5 mm (n = 29) and 14.2 mm (n = 14) for three- and four-extract combinations. No combination approached the 30 mm zone of ketoconazole.

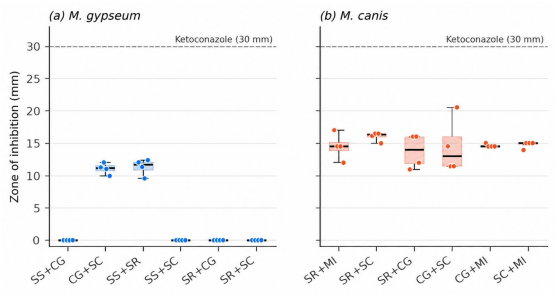

Figure 2. Zones of inhibition of two-extract combinations across the four tested ratios (0.5:0.5, 0.5:1, 1:0.5, 1:1) against (a) *M. gypseum* and (b) *M. canis*. Each point is the mean of triplicate determinations at one ratio; boxes show median and interquartile range, whiskers 1.5 × IQR. Dashed line: ketoconazole (25 µg/mL). SR, *Senegalia rugata*; SS, *Senna siamea*; SC, *Syzygium cumini*; CG, *Calotropis gigantea* ; MI, *Mangifera indica*.

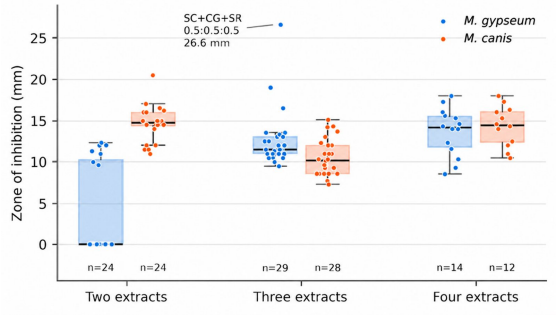

Figure 3. Distribution of mean zones of inhibition by number of extracts in the combination. Points are ratio-level means (each from triplicates); n gives the number of combination–ratio pairs. The largest single value (26.6 mm, *S. cumini* + *C. gigantea* + *S. rugata*, 0.5:0.5:0.5, against *M. gypseum*) is labelled.

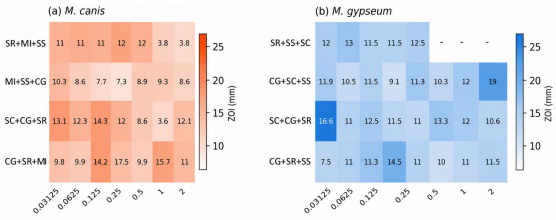

Figure 4. Heat maps of mean zones of inhibition (mm) for three-extract combinations across ratios (relative parts of each extract, in the order listed) against (a) *M. canis* and (b) *M. gypseum*. "–", not tested. †SP and SS are not defined in the original data sheets (see Tables 3 and 4).

GC–MS profile of the synergistic combinations

GC–MS analysis of combination 1 (*S. rugata* + *M. indica*) identified 17 phytoconstituents (Table 8; Supplementary Figure S1). The major peak (13.38%, RT 15.673 min) is as cyclopentanecarboxylic acid with RT 15.905 min, M^+ m/z 156, base peak m/z 110) 3-

Heptenoic acid (6.15%), oleic acid (2.49%), vitamin E (1.64%) and linoleic acid (1.28%) were also prominent, giving a profile rich in fatty acids and antioxidant compounds (Figure 6a). Cyclononasiloxane (3.67%) is a common column-bleed artefact and is not regarded as a plant constituent.

Combination 2 (*C. gigantea* + *S. rugata* + *M. indica*) gave a profile dominated by terpenoids; the GC-MS chromatogram identified 43 compounds). Lupeol (14.26%) and phytol (13.49%) were the major constituents, followed by 13-docosenamide (5.26%), 9,12,15-octadecatrienoic acid ethyl ester (4.00%), lup-20(29)-en-3-ol acetate (3.84%), squalene (3.74%) and ergost-5-en-3-ol (3.66%) (Table 9; Figure 6b; Supplementary Figures S3 and S4).

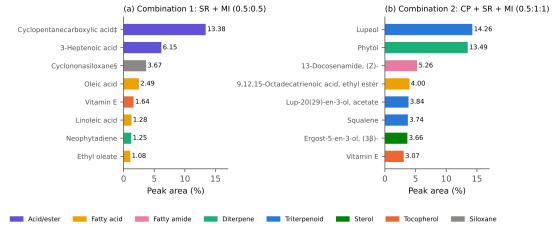

Figure 6. Major GC–MS constituents (≥ 1% peak area) of (a) combination 1 and (b) combination 2, coloured by chemical class. ‡Identity to be confirmed (see text). §Siloxane, probable column-bleed artefact.

Molecular docking

In combination 1, stigmasterol (−11.0 kcal/mol) and lup-20(29)-en-3-one (−8.6 kcal/mol) showed the strongest binding affinities towards the target protein, followed by vitamin E (−7.7 kcal/mol) and phytol (−7.5 kcal/mol) (Figure 7). Linoleic acid bound more weakly (−7.0 kcal/mol) but formed the largest number of hydrogen bonds (three) with active-site residues HIS A:381, SER A:382 and MET A:509, which points to a specific, well-anchored pose despite its moderate score (Supplementary Figure S5).

Combination 2 possessed more high-affinity ligands. Its triterpenoid and sterol constituents, stigmasterol (−11.0 kcal/mol), lupeol (−10.4 kcal/mol), ergost-5-en-3-ol (−10.2 kcal/mol) and tocopherol (−9.8 kcal/mol), bound most strongly, while 13-docosenamide (−7.2 kcal/mol) formed hydrogen bonds with ARG A:385 and HIS A:468 (Figure 7; Supplementary Figure S6). Four of the five top-ranked ligands in combination 2 scored below −9.5 kcal/mol, against only one in combination 1.

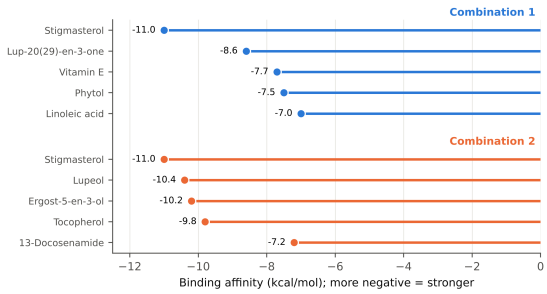

Figure 7 Predicted binding affinities (AutoDock Vina, kcal/mol) of the top-ranked GC–MS constituents of combinations 1 and 2 against lanosterol 14α-demethylase(4LXJ).

Drug-likeness and predicted toxicity

Neric acid (combination 1) and succinic acid (combination 2) satisfied all four Lipinski criteria (Table 10; Figure 8). Oleic acid, linoleic acid, tetradecanoic acid and 13-docosenamide each exceeded the LogP threshold of 5, which is expected for long-chain fatty acids and amides; with a single violation each, all six compounds remain within the rule-of-five allowance. ADMETlab 3.0 flagged neric, oleic and linoleic acids for skin sensitisation, eye corrosion/irritation and respiratory toxicity, while predicting them non-toxic for hERG blockade, DILI, AMES mutagenicity, carcinogenicity and cytotoxicity. Neric acid showed comparatively fewer concerns overall. In combination 2, succinic acid had the cleanest profile, with only eye irritation/corrosion flagged. Tetradecanoic acid also carried skin-sensitisation and respiratory flags, and 13-docosenamide, despite good binding (−7.2 kcal/mol), showed the most toxic endpoints of the three, including hERG blockade and cytotoxicity.

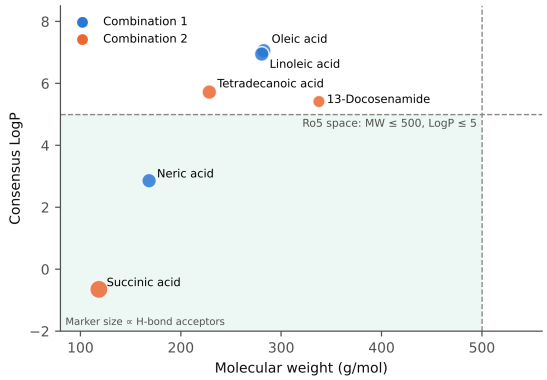

Figure 8. Drug-likeness space of selected constituents (molecular weight against consensus LogP, SwissADME). The shaded region marks Lipinski limits for MW and LogP; marker size is proportional to hydrogen-bond acceptors.

Cytotoxicity on HaCaT keratinocytes

Both combinations inhibited HaCaT growth in a concentration-dependent manner over 31.25–500 µg/mL (Figure 9). Combination 1 inhibited growth by about 22% at 31.25 µg/mL and about 75% at 500 µg/mL, with an IC_{50} of 91.76 µg/mL. Combination 2 followed an almost identical curve with an IC_{50} of 105 µg/mL . Inhibition plateaued below that of doxorubicin (≈96%). Cells treated at 31.25–125 µg/mL kept the spindle-shaped morphology of untreated controls, while rounded, detached cells became more frequent at 250–500 µg/mL (Figure 10).

Set against the antifungal data, these numbers matter. The IC_{50} values lie below the MICs of both combinations, giving selectivity indices (IC_{50}/MIC) well under 1 (Table 11). On HaCaT cells, the crude combinations are therefore cytotoxic at concentrations lower than those needed to stop fungal growth.

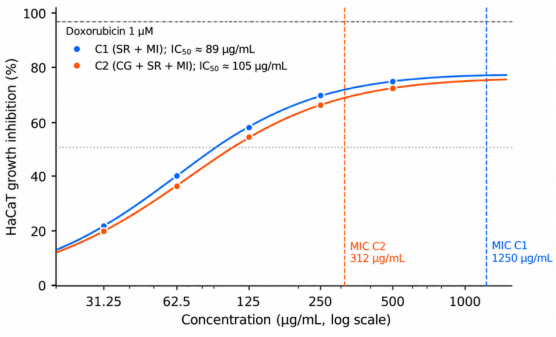

Figure 9. Concentration–response of HaCaT growth inhibition after 48 h exposure to combination 1 (C1) and combination 2 (C2), fitted with a three-parameter log-logistic model. Vertical dashed lines mark the antifungal MIC of each combination against *M. canis*; the horizontal dashed line shows doxorubicin (1 µM).

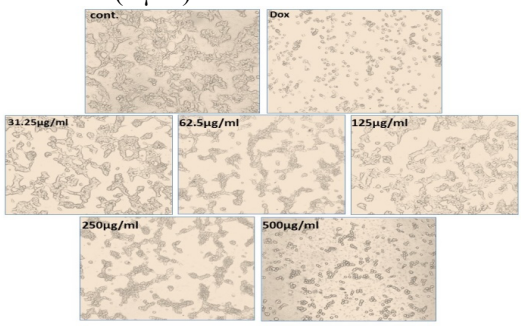

Figure 10. Phase-contrast micrographs of HaCaT cells after 48 h: untreated control, Ketaconazole (1 µM) and combination 1 at 31.25–500 µg/m L.

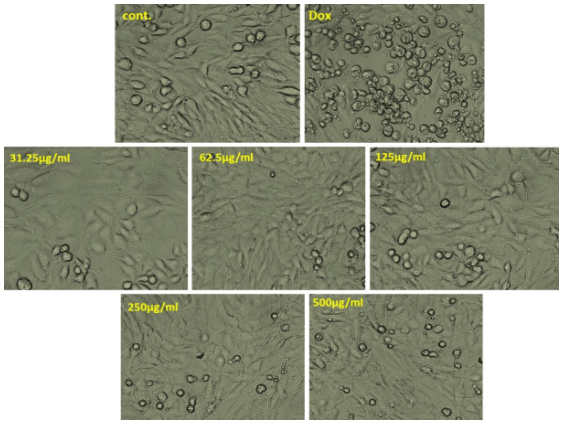

Figure 11: Phase-contrast micrographs of HaCaT cells after 48 h: untreated control, Ketaconazole (1 µM) and combination 2 at 31.25–500 µg/m L.

Discussion

Dermatophytic fungi are the most common fungal organisms infecting skin, nail and hair [3]. In this study the activity of plant-extract combinations differed clearly between *Microsporum canis* and *Microsporum gypseum*, which points to species-dependent responses to the same formulations. Against *M. canis*, *Senegalia rugata* + *Mangifera indica* gave the largest zone among its ratios (17.0 ± 0.7 mm) and was synergistic by FICI. The three-extract combination of *Calotropis gigantea*, *S. rugata* and *M. indica* had the lowest MIC of the series (312 µg/mL) and was also synergistic. Selected combinations can thus show both substantial inhibition and synergy, though these are distinct experimental endpoints.

The contrast with *M. gypseum* is instructive. *S. cumini* + *C. gigantea* + *S. rugata* produced the largest zone of the study against this organism (26.6 ± 2.8 mm) yet showed no synergy, and its MIC (625 µg/mL) was no lower than that of much weaker combinations. A large zone alone does not establish synergy: zone size also depends on how readily constituents diffuse through agar, which favours small polar molecules over the lipophilic triterpenoids and fatty acids that dominated our GC–MS profiles. It is equally clear that an interaction seen against one dermatophyte should not be assumed for another. The two organisms differ ecologically—*M. canis* is zoophilic and *M. gypseum* (*N. gypsea*) geophilic [4, 8]—and may differ in cell-wall and membrane composition, although we did not test this.

Earlier work on antifungal combinations against dermatophytes likewise found that interactions vary with fungal species and with the agents combined [17]. The review by Brescini et al. sets out a useful framework for synergistic, additive and indifferent

interactions and stresses that combinations must be tested experimentally rather than inferred from the activity of single agents [17]. Our data support that view directly. Adding a third or fourth extract did not raise median activity against *M. canis* (Figure 3), and every synergistic outcome depended on a specific ratio. One plausible reason is dilution: at a fixed total concentration, each added extract lowers the share of the most active partner. Antagonistic or simply non-contributing constituents may also mask activity, as described for plant mixtures more generally [15, 16].

The chemistry offers some clues. Both synergistic combinations share *S. rugata* and *M. indica*, and the more potent one adds *C. gigantea*, whose inclusion coincided with a lupeol- and phytol-rich profile and a four-fold lower MIC. Triterpenoids and sterols such as lupeol, stigmasterol and ergost-5-en-3-ol ranked highest in docking. Their binding to lanosterol 14α-demethylase is consistent with a membrane- or sterol-pathway mode of action, but docking scores are predictions only. They do not show that these compounds reach the target in fungal cells, and no single constituent was tested *in vitro*. The docking results should be read as a basis for bioassay-guided fractionation rather than as evidence of mechanism.

The cytotoxicity results temper the antifungal findings. Both combinations reached 50% inhibition of HaCaT growth at about 90–105 µg/mL, three- to twelve-fold below their MICs against *M. canis* (Table 11). HaCaT monolayers are more sensitive than intact, keratinised skin, and 48 h continuous exposure is a severe test, so these values probably overstate the risk of topical use [27]. Even so, a selectivity index below 1 is a serious limitation for crude extracts, and it is the main reason we regard these combinations as leads rather than candidates. The ADMET predictions point the same way: several abundant constituents were flagged for skin sensitisation and irritation, which matters for a product applied to inflamed skin.

Several limitations should be stated. Only one reference strain of each species was tested, and clinical isolates, including azole-resistant *Trichophyton* strains of current concern [11], were not included. The FICI classification depends on the MICs of the individual extracts, which should be reported with the combination MICs (Table 7). GC–MS detects only volatile and semi-volatile compounds, so polar constituents such as phenolics and saponins—abundant in *S. rugata* pods and *M. indica* leaves—were not profiled. Checkerboard assays across a full concentration matrix, time–kill studies and testing on reconstructed skin or *ex vivo* models would strengthen the evidence.

Conclusion

Overall, the present findings identify *S. rugata* + *M. indica* (0.5:0.5) and *C. procera* + *S. rugata* + *M. indica* (0.5:1:1) as promising combinations for further investigation against *M. canis*. Their synergistic interactions, determined by FICI, distinguish them from combinations that inhibited growth without synergy, and none was synergistic against *M. gypseum*. Synergy was set by composition and ratio, not by the number of plants. Because both combinations were cytotoxic to keratinocytes below their MICs, the next step is fractionation to separate the antifungal constituents—particularly the lupeol-, phytol- and sterol-rich fractions of combination 2—from those driving toxicity.

Declarations

Author contributions (CRediT): Mrinalini Devi U.G.: Conceptualization, Investigation, Formal analysis, Writing – original draft. Sharmila T.: Supervision, Methodology, Writing – review & editing. Sushma H.N.: Investigation, Data curation.

Funding: This research received no specific grant from any funding agency

Conflict of interest: The authors declare no conflict of interest.

Ethics statement: Not applicable; the study used reference fungal strains and a commercially obtained human cell line, and involved no human participants or animals.

Data availability: The data supporting the findings of this study are available from the corresponding author on reasonable request.

Acknowledgements: The authors thank the Central Council for Research in Ayurvedic Sciences (CCRAS), Bengaluru, for plant authentication and Bio Edge Solutions GC–MS/MTT.

Tables

Table 1. Antifungal activity (zone of inhibition, mm) of two-extract combinations against *M. gypseum*.

Combination	0.5:0.5	0.5:1	1:0.5	1:1
SS + CG	0	0	0	0
CG + SC	11.3 ± 1.5	12.0 ± 1.5	11.0 ± 1.5	10.0 ± 1.2
SS + SR	12.0 ± 1.2	11.3 ± 0.5	9.6 ± 1.5	12.3 ± 2.0
SS + SC	0	0	0	0
SR + CG	0	0	0	0
SR + SC	0	0	0	0
Ketoconazole (25 µg/mL)	30	—	—	—

Values are mean ± SE (n = 3). SR, *Senegalia rugata* (syn. *Acacia concinna*); SS, *Senna siamea*; SC, *Syzygium cumini*;
CG, *Calotropisgigantea* ; MI, *Mangifera indica*.

Table 2. Antifungal activity (zone of inhibition, mm) of two-extract combinations against *M. canis*.

Combination	0.5:0.5	0.5:1	1:0.5	1:1
SR + MI	17.0 ± 0.7	14.5 ± 0.7	13.5 ± 1.4	14..0 ± 1.2
SR + SC	16.2 ± 1.7	16.5 ± 2.3	12.7 ± 2.3	12.0 ± 1.2
SR + CG	11.0 ± 1.4	16.0 ± 1.8	12 ± 0.9	16.1 ± 1.4
CG + SC	14.5 ± 0.7	11.5 ± 0.7	15.5 ± 0.5	20.5 ± 0.7
CG + MI	15.0 ± 1.4	14.5 ± 0.7	10.7 ± 0.35	14.5 ± 0.7
SC + MI	14.0 ± 1.1	15.0 ± 0.8	14.0 ± 4.0	15.0 ± 0.1
Ketoconazole (25 µg/mL)	30	—	—	—

Values are mean ± SE (n = 3). Asterisks mark values significantly different (one-way ANOVA, Tukey HSD, $p < 0.05$) SR, *Senegalia rugata* (syn. *Acacia concinna*); SS, *Senna siamea*; SC, *Syzygium cumini*; CG, *Calotropis gigantea* ;
MI, *Mangifera indica*.

Table 3. Antifungal activity (zone of inhibition, mm) of three-extract combinations against *M. canis*.

Combination	0.5:0.5:0.5	0.5:0.5:1	0.5:1:0.5	1:0.5:1	1:1:0.5	
SR + MI + SC	11.0 ± 0.9	11.0 ± 0.9	11.0 ± 0.2	12.0 ± 0.0	12.0 ± 0.0	8.6 ± 0.5

Combination	0.5:0.5:0.5	0.5:0.5:1	(.5:1:1	0.5:1:0.5	1:(.5:1	1:1:(.5	
MI+SC+CG	10.3 ± 0.5	8.6 ± 0.5	7.7 ± 0.6	7.3 ± 0.6	9.3 ± 0.5	9.3 ± 0.5	[illegible]
SC+CG+SR	15.1 ± 0.7	12.3 ± 1.1	14.3 ± 1.1	13.0 ± 2.0	9.6 ± 0.5	8.6 ± 0.5	[illegible]
CG+SR+MI	9.6 ± 0.5	8.6 ± 0.5	14.2 ± 2.0	10.3 ± 0.5	8.6 ± 0.5	13.7 ± 0.6	[illegible]

Values are mean ± SE (n = 3 SR, *Senegalia rugata* (syn. *Acacia concinna*); SS, *Senna siamea*; SC, *Syzygium cumini*; CG, *Calotropis gigantea* MI, *Mangifera indica*.

Table 4. Antifungal activity of three-extract combinations against *M. gypseum* (zone of inhibition, mm).

Combination	0.5:0.5:0.5	(.5:(.5:1	(.5:1:(.5	1:(.5:(.5		
SR+SS+SC	12.0 ± 1.4	13.0 ± 1.0	[illegible]	11.5 ± 0.7	12.5 ± 0.7	[illegible]
SS+SC+SS	11.5 ± 0.7	10.5 ± 0.7	[illegible]	9.5 ± 0.7	13.5 ± 0.7	[illegible]
SC+CG+SR	26.6 ± 2.8	11.0 ± 0.5	[illegible]	10.5 ± 0.7	11.0 ± 1.5	[illegible]

Combination	0.5:0.5:0.5:1	(0.5:0.5:1:0.5	1:(0.5:(0.5	
CG + SR + SS	11 ± 0.7	11.0 ± 0.5	16 ± 0.7	11 ± 0.5	(± 0.4	(±

Values are mean ± SE (n = 3); —, not tested.
SR, *Senegalia rugata* (syn. *Acacia concinna*); SS, *Senna siamea*; SC, *Syzygium cumini*; CG, *Calotropis gigantea* ; MI, *Mangifera indica*.

Table 5. Antifungal activity (zone of inhibition, mm) of four-extract combinations (SR + MI + SC + CG against *M. canis*.

No.	Ratio (SR:MI:SC:CG)	Zone of inhibition (mm)
1	1:1:1:1	11.0 ± 0.5
2	0.5:1:1:1	12.5 ± 0.5
3	0.5:0.5:1:1	10.5 ± 0.5
4	1:1:0.5:1	12.0 ± 1.0
5	0.5:0.5:0.5:0.5	16.3 ± 0.5*
6	1:0.5:0.5:0.5	-
7	0.5:1:0.5:0.5	12.6 ± 0.5
8	0.5:0.5:0.5:1	13.6 ± 0.5
9	1:1:0.5:0.5	13.0 ± 1.0
10	1:0.5:0.5:1	13.6 ± 0.5
11	0.5:1:1:0.5	11..6 ± 0.5
12	0.5:0.5:1:0.5	11.6 ± 0.5

Values are mean ± SE (n = 3). SR, *Senegalia rugata* (syn. *Acacia concinna*); SS, *Senna siamea*; SC, *Syzygium cumini*;
CG, *Calotropis gigantea*; MI, *Mangifera indica*.

Table 6.
Antifungal activity (zone of inhibition, mm) of four-extract combinations (SR + SS + SC + CG) against
M. gypseum.

No.	Ratio (SR:SS:SC:CG)	Zone of inhibition (mm)
1	1:1:1:1	15.6 ± 3.5
2	0.5:1:1:1	10.3 ± 0.5
3	0.5:0.5:1:1	8.6 ± 0.5
4	1:1:0.5:1	12.3 ± 0.5
5	0.5:0.5:0.5:0.5	14.0 ± 1.0
6	1:0.5:0.5:0.5	14.3 ± 1.5
7	0.5:1:0.5:0.5	16.0 ± 2.0
8	0.5:0.5:1:0.5	9.3 ± 0.5
9	0.5:0.5:0.5:1	15.3 ± 1.5
10	1:1:0.5:0.5	18.0 ± 1.0*
11	1:0.5:0.5:1	14.6 ± 3.0
12	0.5:1:1:0.5	17.3 ± 1.1
13	0.5:0.5:1:0.5	14.0 ± 1.0

Values are mean ± SE (n = 3).. SR, *Senegalia rugata* (syn. *Acacia concinna*); SS, *Senna siamea*; SC, *Syzygium cumini*;
CG, *Calotropis gigantea*; MI, *Mangifera indica*.

Table 7. Interaction of selected extract combinations by fractional inhibitory concentration index (FICI).

Organism	Combination	Ratio	MIC in combination (µg/mL)	I	Interaction
M. gypseum	CP + SC	0.5:1	625	1	Additive

Organism	Combination	Ratio	MIC in combination (µg/mL)	FICI	Interaction
M. gypseum	SS + SR	1:1	625	1.24	Indifferent
M. gypseum	SC + CP + SR	0.5:0.5:0.5	625	1.99	Indifferent
M. gypseum	SS + SC + CP	1:1:1	312	2.5	Indifferent
M. gypseum	SR + SS + SC + CG	0.5:1:1:0.5	625	2.24	Indifferent
M. canis	SR + MI	0.5:0.5 1250		0.18	Synergistic
M. canis	SR + SC	0.5:1 625			Additive
M. canis	SC + CG + SR	0.5:0.5:0.5	312	1.75	Indifferent
M. canis	CG + SR + MI	0.5:1:1	312	0.49	**Synergistic**
M. canis	SR + MI + SC + SS	0.5:0.5:0.5:0.5	625	1.12	Indifferent

Synergistic, FICI ≤ 0.5; additive, > 0.5–1.0; indifferent, > 1.0–4.0; antagonistic, > 4.0. SR , *Senegalia rugata* (syn. *Acacia concinna*); SS, *Senna siamea*; SC, *Syzygium cumini*; CG, *Calotropis gigantea* ; MI, *Mangifera indica*.

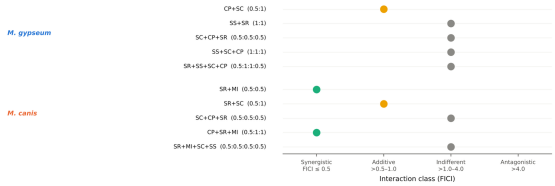

Figure 5: FICI interaction class of the ten combinations taken forward, by organism. Only two combinations, both against *M. canis*, met the synergy criterion.

Table 8. GC–MS profile of combination 1 (*S. rugata* + *M. indica*, 0.5:0.5).

Sl. No.	RT (min)	Peak area (%)	Compound	Formula	MW (g/mol)
1	8.250	0.97	2-Furancarboxaldehyde	$C_5H_4O_2$	96.08
2	13.257	0.44	Pyrrolidine	C_4H_9N	71.12
3	13.448	6.15	3-Heptenoic acid	$C_7H_{12}O_2$	128.17
4	15.673	13.38	Cyclopentanecarboxylic acid	$C_6H_{10}O_2$	114.14
5	18.526	0.39	Safrole	$C_{10}H_{10}O_2$	162.19
6	21.385	0.14	Neric acid	$C_{10}H_{16}O_2$	168.23
7	28.305	0.26	Diethyl L-tartrate	$C_8H_{14}O_6$	206.19
8	31.601	1.25	Neophytadiene	$C_{20}H_{38}$	278.52
9	36.851	0.94	Phytol	$C_{20}H_{40}O$	296.54
10	37.114	0.22	Methyl stearate	$C_{19}H_{38}O_2$	298.51
11	37.351	2.49	Oleic acid	$C_{18}H_{34}O_2$	282.46
12	37.727	1.28	Linoleic acid	$C_{18}H_{32}O_2$	280.45
13	37.837	1.08	Ethyl oleate	$C_{20}H_{38}O_2$	310.52
14	52.243	1.64	Vitamin E	$C_{29}H_{50}O_2$	430.71

	RT (min)	Peak area (%)	Compound	Formula	MW (g/mol)
	52.837	3.67	Cyclononasiloxane, octadecamethyl-[a]	$C_{18}H_{54}O_9Si_9$	667.39
	53.347	0.46	Lup-20(29)-en-3-one	$C_{30}H_{48}O$	424.71
	54.173	0.85	Stigmasterol	$C_{29}H_{48}O$	412.70

RT, retention time; MW, molecular weight. [a]Probable column-bleed artefact.

Table 9. Selected compounds identified by GC–MS in combination 2 (*C. procera* + *S. rugata* + *M. indica*, 0.5:1:1).

No.	RT (min)	Compound	Peak area (%)	Similarity (%)
1	30.049	Tetradecanoic acid	2.65	96
2	31.595	Neophytadiene	1.35	97
3	33.343	Hexadecanoic acid, methyl ester	1.76	95
4	36.847	Phytol	13.49	98
5	37.722	Linoleic acid ethyl ester	1.34	94
6	37.838	9,12,15-Octadecatrienoic acid, ethyl ester	4.00	92
7	44.818	Lupeol	14.26	96
8	47.411	13-Docosenamide, (Z)-	5.26	95
9	48.120	Squalene	3.74	96
10	49.835	Lup-20(29)-en-3-ol, acetate	3.84	82
11	52.236	Vitamin E	3.07	95
12	53.582	Ergost-5-en-3-ol, (3β)-	3.66	90
13	50.402	Succinic acid	0.48	64

Table 10. Drug-likeness of selected phytocompounds based on Lipinski's rule of five (SwissADME).

Compound	Combination	MW (g/mol, ≤ 500)	LogP (≤ 5)	HBD (≤ 5)	HBA (≤ 10)	Violations
Neric acid	1	168.23	2.864	1	2	0
Oleic acid	1	282.46	7.063	1	2	1 (LogP)
Linoleic acid	1	280.45	6.953	1	2	1 (LogP)
Tetradecanoic acid	2	228.37	5.723	1	2	**1 (LogP)**
13-Docosenamide	2	337.58	5.419	1	1	1 (LogP)
Succinic acid	2	118.09	−0.646	2	4	0

HBD, hydrogen-bond donors; HBA, hydrogen-bond acceptors. Tetradecanoic acid was reported as having 0 violations in the original draft; its LogP of 5.723 exceeds the limit, so one violation is listed here.

Table 11. Cytotoxicity on HaCaT keratinocytes relative to antifungal activity against *M. canis*.

Combination	HaCaT IC_{50} (µg/mL)	MIC vs *M. canis* (µg/mL)	Selectivity index (IC_{50}/MIC)
C1: SR + MI (0.5:0.5)	91.76	1,250	0.07
C2: CP + SR + MI (0.5:1:1)	105	312	0.34

A selectivity index > 1 would indicate preferential antifungal activity.

References

Seebacher C, Bouchara JP, Mignon B. Updates on the epidemiology of dermatophyte infections. Mycopathologia. 2008;166(5–6):335–352. https://doi.org/10.1007/s11046-008-9100-9

Havlickova B, Czaika VA, Friedrich M. Epidemiological trends in skin mycoses worldwide. Mycoses. 2008;51(Suppl 4):2–15. https://doi.org/10.1111/j.1439-0507.2008.01606.x

Hay RJ. Tinea capitis: current status. Mycopathologia. 2017;182(1–2):87–93. https://doi.org/10.1007/s11046-016-0058-8

de Hoog GS, Dukik K, Monod M, Packeu A, Stubbe D, Hendrickx M, et al. Toward a novel multilocus phylogenetic taxonomy for the dermatophytes. Mycopathologia. 2017;182(1–2):5–31. https://doi.org/10.1007/s11046-016-0073-9

Gräser Y, El Fari M, Vilgalys R, Kuijpers AFA, de Hoog GS, Presber W, et al. Phylogeny and taxonomy of the family Arthrodermataceae (dermatophytes) using sequence analysis of the ribosomal ITS region. Med Mycol. 1999;37(2):105–114. https://doi.org/10.1080/02681219980000171

Celestrino GA, Verrinder Veasey J, Benard G, Sousa MGT. Host immune responses in dermatophytes infection. Mycoses. 2021;64(5):477–483. https://doi.org/10.1111/myc.13246

Martinez DA, Oliver BG, Gräser Y, Goldberg JM, Li W, Martinez-Rossi NM, et al. Comparative genome analysis of Trichophyton rubrum and related dermatophytes reveals candidate genes involved in infection. mBio. 2012;3(5):e00259-12. https://doi.org/10.1128/mBio.00259-12

Segal E, Elad D. Human and zoonotic dermatophytoses: epidemiological aspects. Front Microbiol. 2021;12:713532. https://doi.org/10.3389/fmicb.2021.713532

Scarampella F, Zanna G, Peano A, Fabbri E, Tosti A. Dermoscopic features in 12 cats with dermatophytosis and in 12 cats with self-induced alopecia due to other causes: an observational descriptive study. Vet Dermatol. 2015;26(4):282–e63.

Adya KA, Inamadar AC, Palit A, Shivanna R, Deshmukh NS. Light microscopy of the hair: a simple tool to “untangle” hair disorders. Int J Trichology. 2011;3(1):46–56. https://doi.org/10.4103/0974-7753.82124

World Health Organization. Antifungal agents in clinical and preclinical development: overview and analysis. Geneva: World Health Organization; 2025. ISBN 978-92-4-010514-0.

Roy M, Karhana S, Shamsuzzaman M, Khan MA. Recent drug development and treatments for fungal infections. Braz J Microbiol. 2023;54(3):1695–1716. https://doi.org/10.1007/s42770-023-00999-z

Kaur N, Bains A, Kaushik R, Dhull SB, Melinda F, Chawla P. A review on antifungal efficiency of plant extracts entrenched polysaccharide-based nanohydrogels. Nutrients. 2021;13(6):2055. https://doi.org/10.3390/nu13062055

Tiple RH, Jamane SR, Khobragade DS. Antifungal activity of neem leaf extract with Eucalyptus citriodora oil and Cymbopogon martini oil against tinea capitis: an in-vitro evaluation. Cureus. 2024;16(5):e59671. https://doi.org/10.7759/cureus.59671

Vaou N, Stavropoulou E, Voidarou CC, Tsakris Z, Rozos G, Tsigalou C, et al. Interactions between medical plant-derived bioactive compounds: focus on antimicrobial combination effects. Antibiotics (Basel). 2022;11(8):1014. https://doi.org/10.3390/antibiotics11081014

van Vuuren S, Viljoen A. Plant-based antimicrobial studies – methods and approaches to study the interaction between natural products. Planta Med. 2011;77(11):1168–1182. https://doi.org/10.1055/s-0030-1250736

Brescini L, Fioriti S, Morroni G, Barchiesi F. Antifungal combinations in dermatophytes. J Fungi (Basel). 2021;7(9):727. https://doi.org/10.3390/jof7090727

18.Savarirajan D, Ramesh VM, Muthaiyan A. In vitro antidermatophytic activity of bioactive compounds from selected medicinal plants. J Anal Sci Technol. 2021;12(1):53. doi: 10.1186/s40543-021-00304-3. Epub 2021 Nov 3. PMID: 34745684; PMCID: PMC8563824.

Clinical and Laboratory Standards Institute. Reference method for broth dilution antifungal susceptibility testing of filamentous fungi; approved standard – second edition. CLSI document M38-A2. Wayne, PA: CLSI; 2008.

Clinical and Laboratory Standards Institute. Method for antifungal disk diffusion susceptibility testing of nondermatophyte filamentous fungi; approved guideline. CLSI document M51-A. Wayne, PA: CLSI; 2010.

Fratini F, Mancini S, Turchi B, Friscia E, Pistelli L, Giusti G, et al. A novel interpretation of the fractional inhibitory concentration index: the case Origanum vulgare L. and Leptospermum scoparium J. R. et G. Forst essential oils against Staphylococcus aureus strains. Microbiol Res. 2017;195:11–17. https://doi.org/10.1016/j.micres.2016.11.005

Dallakyan S, Olson AJ. Small-molecule library screening by docking with PyRx. Methods Mol

Biol. 2015;1263:243–250. https://doi.org/10.1007/978-1-4939-2269-7_19

Trott O, Olson AJ. AutoDock Vina: improving the speed and accuracy of docking with a new scoring function, efficient optimization, and multithreading. J Comput Chem. 2010;31(2):455–461. https://doi.org/10.1002/jcc.21334

Lipinski CA, Lombardo F, Dominy BW, Feeney PJ. Experimental and computational approaches to estimate solubility and permeability in drug discovery and development settings. Adv Drug Deliv Rev. 2001;46(1–3):3–26. https://doi.org/10.1016/S0169-409X(00)00129-0

Daina A, Michielin O, Zoete V. SwissADME: a free web tool to evaluate pharmacokinetics, drug-likeness and medicinal chemistry friendliness of small molecules. Sci Rep. 2017;7:42717. https://doi.org/10.1038/srep42717

Fu L, Shi S, Yi J, Wang N, He Y, Wu Z, et al. ADMETlab 3.0: an updated comprehensive online ADMET prediction platform enhanced with broader coverage, improved performance, API functionality and decision support. Nucleic Acids Res. 2024;52(W1):W422–W431. https://doi.org/10.1093/nar/gkae236

Mosmann T. Rapid colorimetric assay for cellular growth and survival: application to proliferation and cytotoxicity assays. J Immunol Methods. 1983;65(1–2):55–63. https://doi.org/10.1016/0022-1759(83)90303-4

Boukamp P, Petrussevska RT, Breitkreutz D, Hornung J, Markham A, Fusenig NE. Normal keratinization in a spontaneously immortalized aneuploid human keratinocyte cell line. J Cell Biol. 1988;106(3):761–771. https://doi.org/10.1083/jcb.106.3.761

Supplementary material

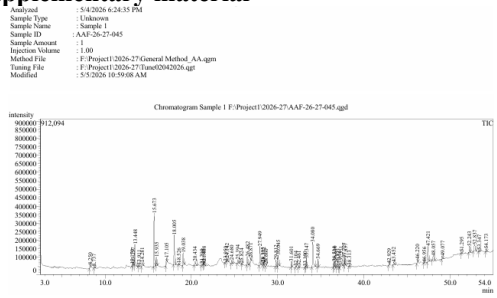

Figure S1. GC–MS total ion chromatogram of combination 1 (*S. rugata* + *M. indica*).

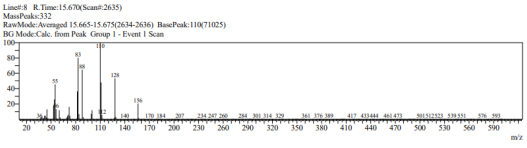

Figure S2. Mass spectrum of the peak at RT 15.905 min in combination 1 (M^+ m/z 156; base peak m/z 110).

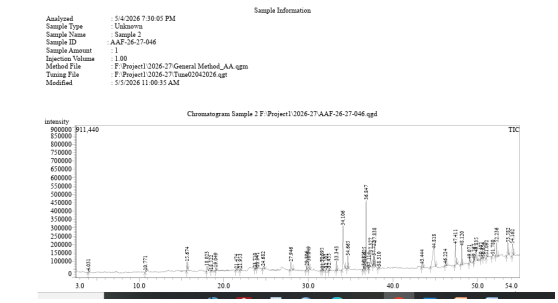

Figure S3. GC–MS total ion chromatogram of combination 2 (*C. procera* + *S. rugata* + *M. indica*).

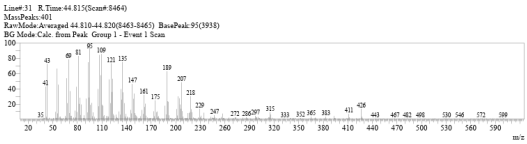

Figure S4. Mass spectrum of lupeol (RT 44.815 min), the most abundant constituent of combination 2.

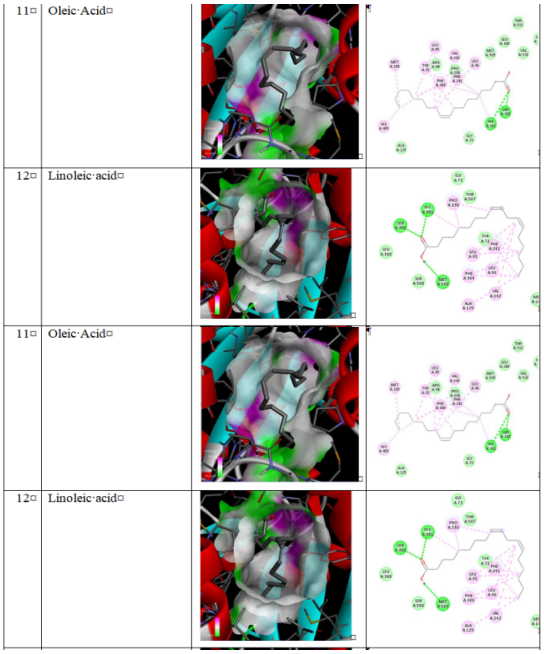

Figure S5. 3D binding pose and 2D interaction diagrams of (a) neric acid, (b) oleic acid and (c) linoleic acid (combination 1) in the active site of lanosterol 14α-demethylase

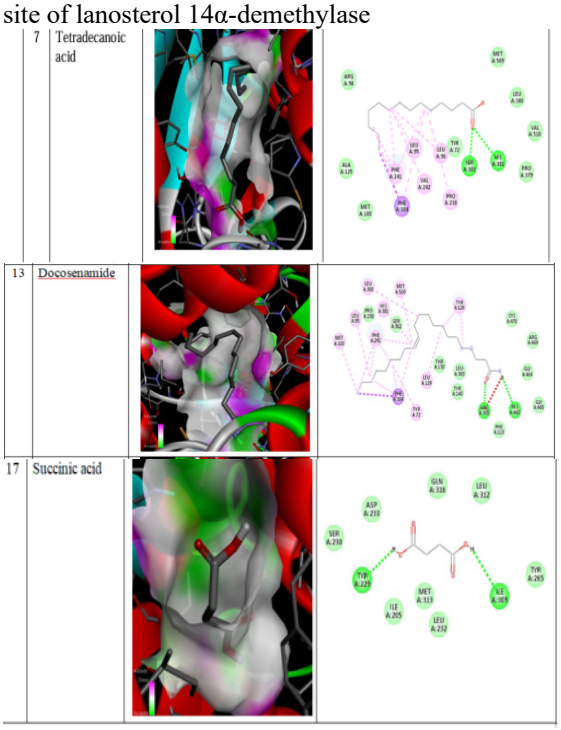

Figure S6. 3D binding pose and 2D interaction diagrams of (a) tetradecanoic acid, (b) 13-docosenamide and (c) succinic acid (combination 2).